Supplementary Information

High−Performance Overall Water Splitting Based On Amorphous Iron Doped Cobalt Tungstate Via Facile Co-precipitation

*Jin Wu, Renjie Xie, Xiangchen Hu, Zhiwei Nie, Yanuo Shi, Yi Yu and Nan Yang**

School of Physical Science and Technology, ShanghaiTech University, Shanghai, 201210, P. R. China.

The word file include:

Table S6 Comparison of catalytic performance with other reported HER catalysts.

Table S7 Comparison to other reported bifunctional catalysts.

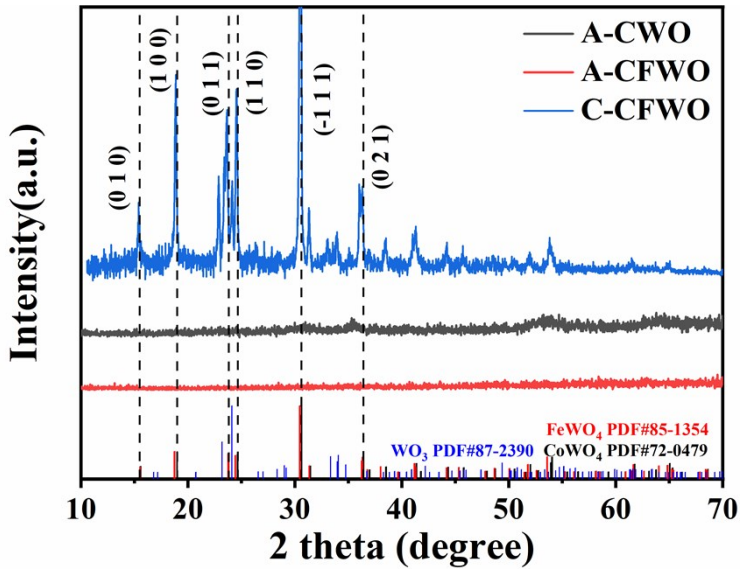

Fig. S1 The XRD diffractograms of A-CWO, A-CFWO and corresponding C-CFWO samples

The Fe 2*p* and W 4*f* spectra were included in Fig. S2. We adapt the fitting parameters of Fe 2p from the ref. 4. The A and B in the main 2p $_{3/2}$ peak are assigned to Fe^{2+} and Fe^{3+}, respectively. The satellite peaks C and D at higher binding energy side are considered to be related to Fe^{2+} and Fe^{3+}, separately. Several constraints are used in order to avoid meaningless fitting. First, the intensity ratio between spin-orbital splitting peaks is assigned to be about two, in agreement with the degeneracy of the spin-orbital split electronic states. Furthermore, the FWHM of peaks is set to be in the range from 2 eV to 4 eV to avoid too broad Gaussian peaks with unphysical meaning. The Fe 2*p* spectrum demonstrates that iron ions are in mixed valence state and confirms the successful incorporation of iron ions in $CoWO_4$. W 4*f* spectra are characterized by 7/2 and 5/2 spin-orbital components. The binding energies correspond to the oxidation state of 6+. No noticeable difference was found for A-CWO and A-CFWO.

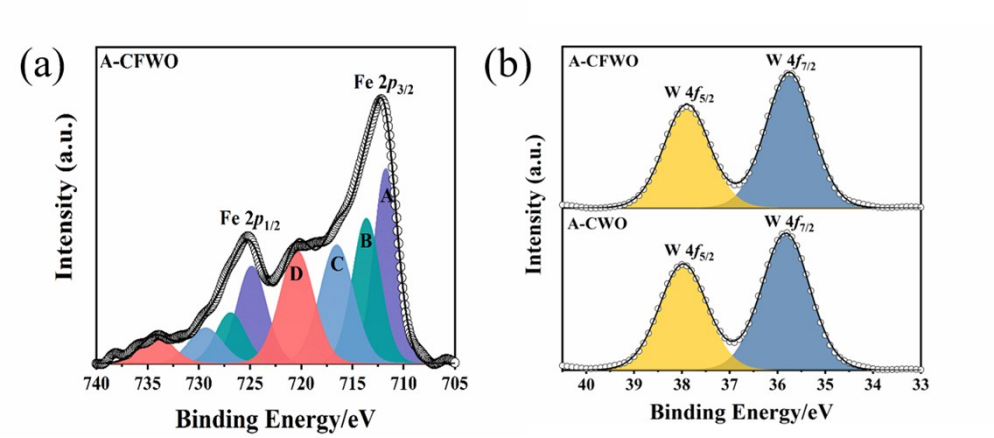

Fig. S2 The XPS spectra of (a) Fe 2*p*, (b) W 4*f* of A-CFWO and A-CWO sample.

Table S1 Comparison of binding energy (BE), FWHM and percentage area of each fitting component of Co $2p_{3/2}$ region in A-CFWO and the A-CWO electrocatalysts.

Peak		**A**	**B**	**C**	**D**	**E**
	BE (eV)	781.52	783.42	785.42	787.92	791.12
A-CFWO	FWHM	2.26	2.50	2.50	3.43	3.50
	Area	1.00	0.64	0.34	0.67	0.24
	BE (eV)	781.50	783.30	785.37	788.00	791.70
A-CWO	FWHM	2.16	2.50	2.32	3.50	3.50
	Area	1.00	0.80	0.33	0.71	0.20

Table S2 Comparison of binding energy (BE), FWHM and area percent of each fitting component of O 1*s* in A-CFWO and the A-CWO electrocatalysts. O_L represents lattice oxygen, O_S represents surface oxygen.

Sample	**A-CFWO**		**A-CWO**	
	O_L	O_S	O_L	O_S
BE (eV)	530.99	531.93	531.06	531.91
FWHM	1.42	2.62	1.47	2.64
Area	1.00	0.41	1.00	0.56

Table S3 Comparison of binding energy (BE), FWHM and area percent of each fitting component of W 4*f* in A-CFWO and the A-CWO electrocatalysts.

Sample	**A-CFWO**		**A-CWO**	
	W $4f_{7/2}$	W $4f_{5/2}$	W $4f_{7/2}$	W $4f_{5/2}$
BE (eV)	35.76	37.90	35.83	37.97
FWHM	1.20	1.17	1.23	1.22
Area	1.00	0.75	1.00	0.77

Table S4 Comparison of binding energy (BE), FWHM and area percent of each fitting component of Fe $2p_{3/2}$ in A-CFWO electrocatalysts.

Sample	**A-CFWO**			
	A	B	C	D
BE (eV)	711.74	713.64	716.54	720.44
FWHM	2.82	3.30	4.00	4.00
Area	1.00	0.87	0.86	0.82

The active surface area of catalysts was calculated from their electrochemical capacitance, which could be measured by cyclic voltammetry. A narrow potential window from 0.92 V to 1.02 V *vs*. RHE with no faradaic processes was measured and the scan rates were 5, 10, 20, 40, 80 and 160 mV s^{-1}, as shown in Fig. S3. Therefore, the current should be expected to be linearly proportional to the active surface area due to the charging of the double layer. Then, the plots of the half of the capacitive current density (ΔJ, $(J_{anodic} - J_{cathodic})/2$) against the scan rate can be plotted, where the slope can be calculated and defined as the double layer capacitance (C_{dl}).

The ECSA of catalysts was further calculated from the C_{dl} according to the following equation: $ECSA = \frac{C_{dl}\,(mF\ cm^{-2})}{C_s\,(mF\ cm^{-2})per\ cm^2}$. The C_{dl} is the double-layer capacitance and Cs per cm^2 is the specific capacitance of a planar surface, which is assigned to be 0.04 mF cm^{-2}, with a standard 1 cm^2 real surface area[1, 2]. The ECSA of A-CFWO, A-CWO and C-CFWO was calculated to be 56.75, 35.25, and 21.75 cm^2.

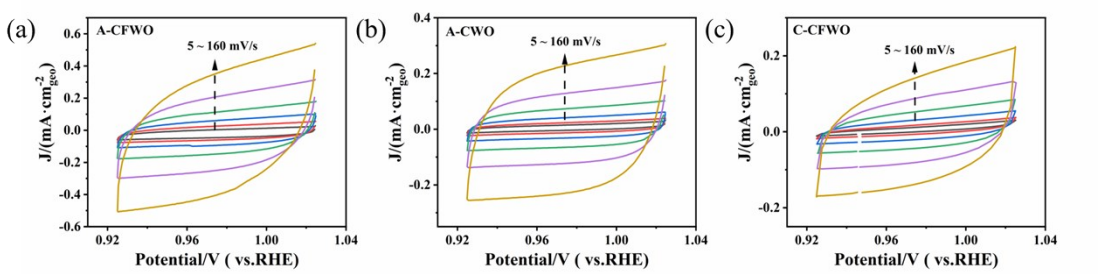

Fig. S3 Cyclic voltammograms of (a) A-CFWO (b) A-CWO (c) C-CFWO measured in the double layer capacitance region 0.92-1.02 V vs. RHE at the scan rates of 5, 10, 20, 40, 80 and 160 mV s^{-1} in 1 M KOH solution.

The comparison of ECSA normalized current density can be found in Fig. S4. As can be seen that the ECSA normalized current density is significantly larger in A-CFWO,

revealing its superior intrinsic activity.

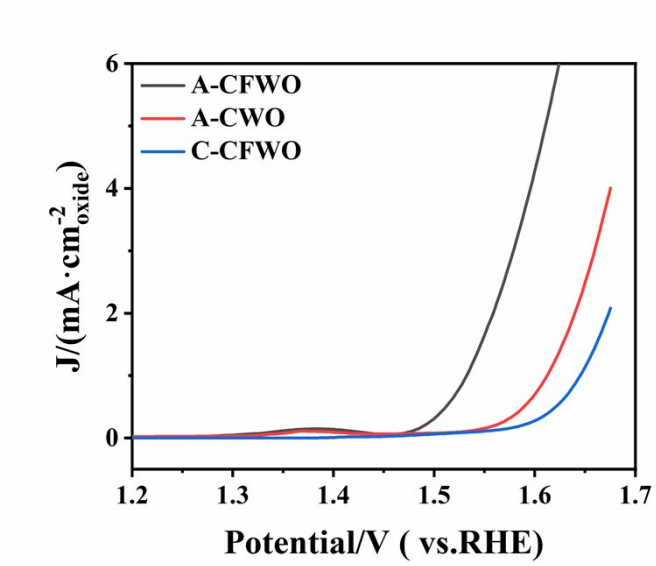

Fig. S4 Polarization curves normalized to the electrochemical active surface area (ECSA).

The XPS peaks of Co 2p and O 1s of the A-CFWO catalyst after the OER test were recorded in Figure S5. The post-OER Co 2p spectra shows a sharpening of the main $2p_{3/2}$ and $2p_{1/2}$ and a dramatic decrease in intensity of the satellite structures, which should be related to a significant increase in the valence state of cobalt[3, 4]. In addition, new features can be clearly seen for O 1s after the OER test. The new peak at around 532 eV was observed and was further deconvoluted to OH and OOH group[5]. Therefore, the appearance of OOH component in O 1s and the higher oxidation state of cobalt in Co 2p indicate the formation of CoOOH layer on the surface of A-CFWO after the OER reaction. Furthermore, the area ratio between Co 2p and W 4f before and after the OER was analyzed and compared. The ratio increases from about 0.8 for as-prepared A-CFWO to about 9.7 for A-CFWO after the OER measurements. In short, the significantly higher area ratio supports the formation of highly active CoOOH layer[6] after the OER measurements for A-CFWO and may explain the origin of its superior OER activity. The post Co 2p and O 1s spectra of A-CFWO after HER are rather similar to those of as-prepared ones. The noticeable differences are the appearance of H_2O (about 536 eV) and the broadening of O 1s, which could be related to the presence of OH group. Therefore, it is reasonable to conclude that A-CFWO shows a high stability for the HER reaction.

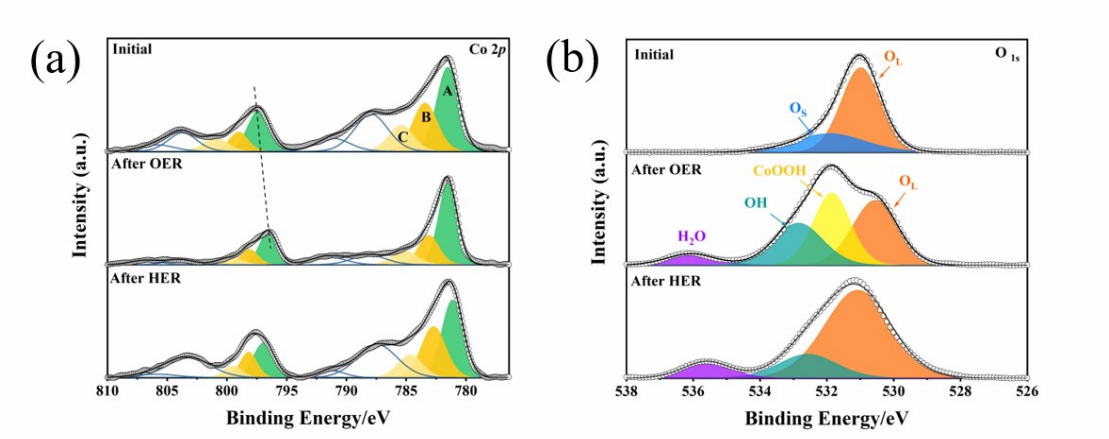

Fig. S5 The XPS spectra of (a) Co 2*p*, (b) O 1*s* of A-CFWO after OER and HER test.

Table S5, S6 and S7 show the OER, HER activity and overall water splitting comparison of A-CFWO with some of most reported state-of-the art electrocatalysts in the literature.

Table S5 Comparison of OER activity of A-CFWO with the literature.

Catalysts	Overpotentia l（η10）	Electrode	Electrolyte	Reference
A-CFWO	259	Ni foam	1M KOH	This Work
$Co_{0.708}Fe_{0.292}WO_4$	327	GCE	1M KOH	7
$CoWO_4$ NPs	336	Ni	1M KOH	8
CoNi-CuHP/NF	299	Ni foam	1M KOH	9
NiCoFeB	284	Ni foam	1M KOH	10
$Ni_{0.75}Fe_{0.125}V_{0.125}$-LDHs	361	Ni foam	1M KOH	11
MoO_2	300	Ni foam	1M KOH	12
$CoWO_{4-x}$@C	295	Carbon paper	1M KOH	13
IrO_2	309	Ni foam	1M KOH	14
FeNi@FeNiB-700	399	Ni foam	1M KOH	15
LCO	381	GCE	1M KOH	16

Note: η10: overpotential at 10 mA cm^{-2}.

Table S6 Comparison of HER acidity of A-CFWO with the literature.

Catalysts	Overpotential （η10）	Electrode	Electrolyte	Reference
A-CFWO	118.2	Ni foam	1M KOH	This Work

Co-Ni_3N	194	GCE	1M KOH	[17]
PNC/Co	289	Ni foam	1M KOH	[18]
CoP nanowire/CC	209	Ni foam	1M KOH	[19]
FeP nanowire arrays	194	Ni foam	1M KOH	[20]
Co-Fe-P	295	Ni foam	1M KOH	[21]
Ni_3S_2-Ni_2P	130	Ni foam	1M KOH	[22]
$NiCo_2S_4$@NiFe LDH	200	Ni foam	1M KOH	[23]
CuCo-Ni_3S_2	204	Ni foam	1M KOH	[24]
3D Ni_3S_2	182	Ni foam	1M KOH	[25]
NiFeS	180	Ni foam	1M KOH	[26]

Note: η10: overpotential at 10 mA cm^{-2}.

GCE: Glassy Carbon Electrode

Table S7 Comparison of overall water splitting performance of A-CFWO with the literature.

Catalysts	Electrolyte	HER vs. RHE (V) @ 10 mA cm^{-2}）	OER vs. RHE (V) @ 10 mA cm^{-2}	Full Water Splitting vs. RHE (V) @ 10 mA cm-2	Reference
A-CFWO	1M KOH	-0.118	1.489	1.55	This Work
Ni_3S_2/NF	1M KOH	-0.223	1.49	1.76	[27]
Ni_5P_4 Films/Ni foil	1M KOH	-0.15	1.56	<1.7	[28]
NiCoP/NF	1M KOH	-0.032	1.51	1.58	[29]
$Ni_{0.69}Co_{0.31}$–P	1M KOH	-0.096	1.496	1.59	[30]
Co_4Ni_1P	1M KOH	-0.129	1.475	1.59	[31]
$NiCo_2S_4$	1M KOH	-0.21	1.49	1.63	[32]
CP/CTs/Co-S	1M KOH	-0.19	1.536	1.743	[33]
$Ni_{1.5}Fe_{0.5}P$	1M KOH	-0.282	1.494	1.635	[34]
Ni/Mo_2C-PC	1M KOH	-0.179	1.598	1.66	[35]
f-CoP/CoP_2/Al_2O_3	1M KOH	-0.066	1.53	1.65	[36]

References:

1. C. C. McCrory, S. Jung, J. C. Peters and T. F. Jaramillo, *J. Am. Chem. Soc.*, 2013, **135**, 16977-16987.
2. L. Yang, H. Ren, Q. Liang, K. N. Dinh, R. Dangol and Q. Yan, *Small*, 2020, **16**, 1906766.

3. S. C. Petitto, E. M. Marsh, G. A. Carson and M. A. Langell, *J. Mol. Catal. A-Chem.*, 2008, **281**, 49-58.
4. Y. Lykhach, S. Piccinin, T. Skala, M. Bertram, N. Tsud, O. Brummel, M. Farnesi Camellone, K. Beranova, A. Neitzel, S. Fabris, K. C. Prince, V. Matolin and J. Libuda, *J. Phys. Chem. Lett.*, 2019, **10**, 6129-6136.
5. Y. Han, S. Axnanda, E. J. Crumlin, R. Chang, B. Mao, Z. Hussain, P. N. Ross, Y. Li and Z. Liu, *J. Phys. Chem. B*, 2018, **122**, 666-671.
6. M. Favaro, J. Yang, S. Nappini, E. Magnano, F. M. Toma, E. J. Crumlin, J. Yano and I. D. Sharp, *J. Am. Chem. Soc.*, 2017, **139**, 8960-8970.
7. W. Shao, Y. Xia, X. Luo, L. Bai, J. Zhang, G. Sun, C. Xie, X. Zhang, W. Yan and Y. Xie, *Nano Energy*, 2018, **50**, 717-722.
8. V. K. V. P. Srirapu, A. Kumar, P. Srivastava, R. N. Singh and A. S. K. Sinha, *Electrochim. Acta*, 2016, **209**, 75-84.
9. Y. Zhang, T. Qu, F. Bi, P. Hao, M. Li, S. Chen, X. Guo, M. Xie and X. Guo, *ACS Sustainable Chem. Eng.*, 2018, **6**, 16859-16866.
10. Y. Li, B. Huang, Y. Sun, M. Luo, Y. Yang, Y. Qin, L. Wang, C. Li, F. Lv, W. Zhang and S. Guo, *Small*, 2019, **15**, 1804212.
11. K. N. Dinh, P. Zheng, Z. Dai, Y. Zhang, R. Dangol, Y. Zheng, B. Li, Y. Zong and Q. Yan, *Small*, 2018, **14**, 1703257.
12. Y. Jin, H. Wang, J. Li, X. Yue, Y. Han, P. K. Shen and Y. Cui, *Adv. Mater.*, 2016, **28**, 3785-3790.
13. F. Luo, R. Xu, S. Ma, Q. Zhang, H. Hu, K. Qu, S. Xiao, Z. Yang and W. Cai, *Appl. Catal. B-Environ.*, 2019, **259**, 118090.
14. Y. Li, T. Zhao, M. Lu, Y. Wu, Y. Xie, H. Xu, J. Gao, J. Yao, G. Qian and Q. Zhang, *Small*, 2019, **15**, 1901940.
15. H. Yuan, S. Wang, X. Gu, B. Tang, J. Li and X. Wang, *J. Mater. Chem. A*, 2019, **7**, 19554-19564.
16. C. Zhao, N. Li, R. Zhang, Z. Zhu, J. Lin, K. Zhang and C. Zhao, *ACS Appl. Mater. Interfaces*, 2019, **11**, 47858-47867.
17. C. Zhu, A. L. Wang, W. Xiao, D. Chao, X. Zhang, N. H. Tiep, S. Chen, J. Kang, X. Wang, J. Ding, J. Wang, H. Zhang and H. J. Fan, *Adv. Mater.*, 2018, **30**, 1705516.
18. X. Li, Z. Niu, J. Jiang and L. Ai, *J. Mater. Chem. A*, 2016, **4**, 3204-3209.
19. J. Tian, Q. Liu, A. M. Asiri and X. Sun, *J. Am. Chem. Soc.*, 2014, **136**, 7587-7590.
20. C. Y. Son, I. H. Kwak, Y. R. Lim and J. Park, *Chem. Commun.*, 2016, **52**, 2819-2822.
21. T. Zhang, J. Du, P. Xi and C. Xu, *ACS Appl. Mater. Interfaces*, 2017, **9**, 362-370.
22. P. Wang, H. He, Z. Pu, L. Chen, C. Zhang, Z. Wang and S. Mu, *Dalton Trans.*, 2019, **48**, 13466-13471.
23. J. Liu, J. Wang, B. Zhang, Y. Ruan, L. Lv, X. Ji, K. Xu, L. Miao and J. Jiang, *ACS Appl. Mater. Interfaces*, 2017, **9**, 15364-15372.
24. J.-F. Qin, M. Yang, S. Hou, B. Dong, T.-S. Chen, X. Ma, J.-Y. Xie, Y.-N. Zhou,

J. Nan and Y.-M. Chai, *Appl. Surf. Sci.*, 2020, **502**, 144172.
25. T. Zhu, L. Zhu, J. Wang and G. W. Ho, *J. Mater. Chem. A*, 2016, **4**, 13916-13922.
26. P. Ganesan, A. Sivanantham and S. Shanmugam, *J. Mater. Chem. A*, 2016, **4**, 16394-16402.
27. L. L. Feng, G. Yu, Y. Wu, G. D. Li, H. Li, Y. Sun, T. Asefa, W. Chen and X. Zou, *J. Am. Chem. Soc.*, 2015, **137**, 14023-14026.
28. M. Ledendecker, S. Krick Calderon, C. Papp, H. P. Steinruck, M. Antonietti and M. Shalom, *Angew. Chem. Int. Ed.*, 2015, **54**, 12361-12365.
29. H. Liang, A. N. Gandi, D. H. Anjum, X. Wang, U. Schwingenschlogl and H. N. Alshareef, *Nano Lett.*, 2016, **16**, 7718-7725.
30. Z. Yin, C. Zhu, C. Li, S. Zhang, X. Zhang and Y. Chen, *Nanoscale*, 2016, **8**, 19129-19138.
31. L. Yan, L. Cao, P. Dai, X. Gu, D. Liu, L. Li, Y. Wang and X. Zhao, *Adv. Funct. Mater.*, 2017, **27**, 1703455.
32. A. Sivanantham, P. Ganesan and S. Shanmugam, *Adv. Funct. Mater.*, 2016, **26**, 4661-4672.
33. J. Wang, H. X. Zhong, Z. L. Wang, F. L. Meng and X. B. Zhang, *ACS Nano*, 2016, **10**, 2342-2348.
34. H. Huang, C. Yu, C. Zhao, X. Han, J. Yang, Z. Liu, S. Li, M. Zhang and J. Qiu, *Nano Energy*, 2017, **34**, 472-480.
35. Z. Y. Yu, Y. Duan, M. R. Gao, C. C. Lang, Y. R. Zheng and S. H. Yu, *Chem. Sci.*, 2017, **8**, 968-973.
36. W. Li, S. Zhang, Q. Fan, F. Zhang and S. Xu, *Nanoscale*, 2017, **9**, 5677-5685.